Ligand-Field Calculations on Pseudo-Tetragonal High-Spin Fe(II) Compounds

Part I: Calculations of paramagnetic susceptibility and electric quadrupole splitting

A. Vermaas, W. L. Groeneveld
Department of Coordination Chemistry, State University, P.O. Box 75, Leiden
The Netherlands

and J. Reedijk
Department of Chemistry, Delft University of Technology, Julianalaan 136, Delft
The Netherlands

(Z. Naturforsch. **32a**, 1393–1403 [1977]; received October 18, 1977)

The paramagnetic susceptibility behaviour as well as the Mössbauer quadrupole splitting are calculated for high-spin d^6 systems with a tetragonal or an orthorhombic point-symmetry. The calculations include a simultaneous perturbation of the ^5D multiplet by spin-orbit interaction and static octahedral-tetragonal and orthorhombic fields. The lattice contribution to the electric-field gradient is calculated on the basis of a crystal-field model that directly relates crystal-field energy parameters to the lattice contribution. It appears that, espacially for compounds with large Ds values, the lattice contribution to the quadrupole splitting cannot be ignored.

Introduction

During recent years many workers have tried to fit either or both experimentally obtained magnetic susceptibilities[1,2,3] and electric quadrupole splittings[4–12] of high-spin iron(II) compounds, using the results of ligand-field calculations concerning the perturbation of the cubic field $^5T_{2g}$ term. A simultaneous action of spin-orbit coupling and axial or orthorhombic ligand field was used as a perturbation on the $^5T_{2g}$ cubic ground state. Gerloch[3] also took into account the mixing with excited quintet states. Although for many high-spin iron(II) compounds energy splitting parameters were eliminated either from magnetic susceptibility data, or from Mössbauer data, only few workers[5,7] compared these data within one theoretical model. Moreover, only a limited number of compounds was investigated. Therefore, we decided to extend the theory on this field into two directions:

i) refining the available theory by including mixing with excited quintet states, orthorhombic crystal fields, and by including a lattice contribution to the quadrupole splitting.

ii) carrying out the calculations on quadrupole splitting and magnetic susceptibility within a single model.

In Part II, the results obtained using this procedure will be compared with experimental data.

Theory

A) Energy Calculations

The basis for the calculations of the paramagnetic susceptibility as well as the quadrupole splitting of iron(II) high spin compounds, is formed by the calculation of the energy levels and the corresponding eigenfunctions. These calculations involve a diagonalization of the energy matrix of the states originating from the ^5D multiplet, written in $|L, M_L, S, M_S\rangle$ quantization. This multiplet is perturbed by a crystalfield Hamiltonian and by spin-orbit coupling effects:

$$\hat{H} = V_{\text{c.f.}} + \sum_i \zeta\, l_i s_i\,. \tag{1}$$

Since only basis functions of the ^5D multiplet are considered, the spin-orbit interaction can be written as:

$$\hat{H}_{\text{s.o.}} = \lambda \hat{L} \hat{S} \tag{2}$$

where $\lambda = -\zeta/4$.

Reprint requests to Dr. J. Reedijk, Department of Chemistry, Delft University of Technology, Julianalaan 136, *Delft/Niederlande.*

In order to develop a theory with a wide range of applicability, a crystal-field Hamiltonian is chosen such that it satisfies an orthorhombic symmetry (pointgroup D_{2h}):

$$\hat{V}_{\text{c.f.}} = \hat{V}_{\text{octahedral}} + \hat{V}_{\text{tetragonal}} + \hat{V}_{\text{orthorhombic}} \,. \tag{3}$$

With the aid of the method given by Hutchings[13] and after evaluating the radial integrals of the matrix elements of the energy matrix, a crystal-field Hamiltonian can be obtained that is acting on the angular parts of the wavefunctions:

$$\begin{aligned} \hat{V}'_{\text{c.f.}} &= Dq^{xy}(O_4^0 + 5.O_4^4)/12 \qquad (4) \\ &+ Ds.O_2^0/3 - Dt.O_4^0/12 + Dz.O_2^2/3 - Dv.O_4^2/12 \,. \end{aligned}$$

In this expression Dq^{xy}, Ds and Dt have their usual meaning[14]; the coefficients of O_2^2 and O_4^2 are chosen such that

$$\begin{aligned} &\langle L_z = \mp 1 \,|\, Du.O_2^2/3 - Dv.O_4^2/12 \,|\, L_z = \pm 1 \rangle \\ &\quad = Du + Dv \,. \end{aligned} \tag{5}$$

This Hamiltonian does neither take into account anisotropic spin-orbit interaction[15, 16], nor vibronic coupling, nor intraionic spin-spin coupling. Especially for systems close to cubic symmetry, vibronic coupling influences markedly the paramagnetic susceptibility[17, 18, 19, 20]. Intraionic spin-spin coupling was used as an additional part of the Hamiltonian by Sams[21]. We believe that this energy contribution will be negligebly small, because the $(3d)^6$ configuration has no other multiplets having the same spin multiplicity as the ^{5}D multiplet. Therefore the intraionic spin-spin coupling energy will be of the same order of magnitude as the zero-field splitting in high-spin Mn(II) compounds, and thus very small[22, 23, 24] with respect to the energy separations between the populated levels that arise by the action of the perturbation Hamiltonian as denoted in (1).

B) Quadrupole Splitting

The interaction of an electric-field gradient (EFG) tensor with the quadrupole moment Q of a $^{57\text{m}}$Fe nucleus, results in a quadrupole splitting ΔE_Q[25]:

$$\Delta E_Q = \tfrac{1}{2} e^2 q\, Q (1 + \eta^2/3)^{1/2} \tag{6}$$

in which q and η have their usual meaning[4]. Although the quadrupole moment Q is a natural constant, the reported values varied significantly up to 1970[4, 26–31]. The last few years the reported data are close to 0.20 barn[32, 33]. Therefore the value of 0.20 barn has been used in our calculations. The components of the electric field gradient tensor are given by:

$$\partial^2 V/\partial r_i\, \partial r_j = -\sum_k Z_k (3\, r_{ik}\, r_{jk} - \delta_{ij}\, r_k^2)/r_k^5 \tag{7}$$

in which r_i, $r_j = x, y, z$, Z is the charge of a particle (nucleus or electron), and r is the distance to the ^{57}Fe nucleus considered. The summation should be performed over all charges in the lattice, except the considered ^{57}Fe nucleus itself. According to the symmetry adapted in our calculations, there are no off-diagonal elements of the EFG tensor, so that no transformations of the axes have to be performed for the calculation of q and η.

Following others[4, 9] the charges in (7) are divided into two classes:

1) The electrons of the $3d$ shell of the iron nucleus, resulting in the "valence contribution", q_{val} and η_{val}.
2) All other charges in the lattice, resulting in the "lattice contribution", q_{lat} and η_{lat}.

Therefore:

$$q = q_{\text{val}} + q_{\text{lat}} \tag{8}$$

and

$$\eta = \eta_{\text{val}} + \eta_{\text{lat}} \,. \tag{9}$$

q_{val} and η_{val} have been calculated as the ensemble average over the 25 eigenvectors:

$$q_{\text{val}} = \frac{\sum_{i=1}^{25} \langle q_{\text{val}} \rangle_i \exp\{-E_i/k\,T\}}{\sum_{i=1}^{25} \exp\{-E_i/k\,T\}} \,, \tag{10}$$

$$\eta_{\text{val}} = \frac{\sum_{i=1}^{25} \langle \eta_{\text{val}} \rangle_i \exp\{-E_i/k\,T\}}{\sum_{i=1}^{25} \exp\{-E_i/k\,T\}} \,. \tag{11}$$

In the calculation of q_{val} and η_{val} it has been assumed that there is no anisotropic mixing between $3d$ orbitals and ligand orbitals and furthermore that all five $3d$ metal orbitals have the same $\langle r^{-3} \rangle_{3d}$ value. For $(1 - R)\, \langle r^{-3} \rangle_{3d}$, the data as calculated by Freeman and Watson[34] for the free-ion are used. This free-ion value is in good agreement with experimentally determined ones[35, 36, 37], and results in a maximum valence contribution to the quadrupole splitting of 3.8 mm/s. In the past some investigators calculated the lattice contribution to the quadrupole splitting, either by applying a lattice summation[26] in a point-charge model, or by using the analogy that exists between this lattice contribution and the second-order crystal-field energy distortion parameters[4, 9, 38].

Both approximations are thus based on an electrostatic concept with respect to the crystal lattice. Moreover the lattice summation in which ions are assumed to be point charges, includes the presupposition that the charge distribution of the ions is spherically symmetric. Only in that case the electric field gradient at a point outside the charge distribution can be thought to originate from a point charge at the center of that charge distribution. The difference between the real electric field gradient of an ion, and the electric field gradient calculated from a point-charge model, can therefore be considerable, especially for the contributions of the ions nearest to the ^{57}Fe nucleus. Therefore, we decided not to rely on such lattice summations, but to use a modified version of the method introduced by Ingalls[4]. According to Ingalls, only second-order energy distortion parameters are important in the energy calculations, so that there is a direct relation between the ground-state splitting and q_{lat} and η_{lat}. We now include also Dt and Dv in the electron energy calculations, because Dt has shown to be significant and may even reverse the ground-state energy levels[39].

Using a crystal-field concept, there is a direct relation between the second-order crystal-field splitting parameters Ds and Du and the lattice contribution to the quadrupole splitting q_{lat} and η_{lat}:

$$q_{\text{lat}} = (1 - \gamma_\infty)\, 14\, Ds/(e^2 \langle r^2 \rangle_{3d}) \,, \tag{12}$$

$$q_{\text{lat}}\, \eta_{\text{lat}} = -\, (1 - \gamma_\infty)\, 14\, Du/(e^2 \langle r^2 \rangle_{3d}) \,. \tag{13}$$

With $\gamma_\infty = -9.14$[37] and $\langle r^2 \rangle_{3d} = 0.392$ A^2[34], this results in:

$$\tfrac{1}{2}\, e^2 q_{\text{lat}}\, Q = 0.937\, Ds/10^3 \text{ mm/s} \tag{14}$$

and

$$\tfrac{1}{2}\, e^2 q_{\text{lat}}\, \eta_{\text{lat}}\, Q = -\, 0.937\, Du/10^3 \text{ mm/s} \tag{15}$$

in which the energy parameters Ds and Du are expressed in cm^{-1}.

As mentioned above, Eqs. (14) and (15) have been derived within a crystal-field model. From the interpretation of Dq[40], it is clear that the origin of deduced crystal-field energy parameters is not basicly electrostatic. Therefore the proportional constants in (14) and (15) are not unambigious. Nevertheless, previous work[9, 38], using (14), showed fair agreement with experiment. Moreover (14) and (15) permit a calculation of the quadrupole splitting that is very easy to handle. Therefore, this method will be used in our calculations, although it must be kept in mind that (14) and (15) are not strict relations. However, within that framework it is possible to discuss the trends of quadrupole-splitting values of a series of compounds, although it may be insufficient for an exact approach of a single compound.

C) Paramagnetic Susceptibility

The molar paramagnetic magnetization M in the direction of an applied magnetic field $\boldsymbol{H}$ is given by the expression

$$M = -\, N \frac{\sum\limits_p (\mathrm{d}E_p/\mathrm{d}H) \exp(-\, E_p/k\,T)}{\sum\limits_p \exp(-\, E_p/k\,T)} \,. \tag{16}$$

It has been shown[41, 42] that for magnetic fields H, with $\beta H/k\,T \ll 1$, the powder magnetization is given by

$$M_{\text{powder}} = (M_x + M_y + M_z)/3 \tag{17}$$

where x, y and z denote the three molecular axes. The paramagnetic suceptibility tensor χ reduces to a tensor with only diagonal terms for systems with orthogonal molecular axes, so that the molar susceptibility

$$\chi_{mm} = M_m/H \tag{18}$$

and the magnetic moment

$$\mu_m = \{(3\,k\,T\,\chi_{mm})/(N\,\beta^2)\}^{1/2} \tag{19}$$

where m stands for molecular axes x, y or z.

Furthermore, for $\beta H/k\,T \ll 1$, χ_{mm} can be calculated in good approximation by Van Vleck's formula

$$\chi_{mm} = N \frac{\sum\limits_p ((E^{(1)}_{p,m})^2/k\,T - 2\, E^{(2)}_{p,m}) \exp\{-\, E^{(0)}_p/k\,T\}}{\sum\limits_p \exp(-\, E^{(0)}_p/k\,T)} \tag{20}$$

where $E^{(0)}_p$ is the energy of the p'th level in the absence of a magnetic field,

$$E^{(1)}_{p,m} = \langle \psi_p \,|\, \hat{\mu}_m \,|\, \psi_p \rangle \,,$$

$$E^{(2)}_{p,m} = \sum_{p'} \frac{|\langle \psi_p \,|\, \hat{\mu}_m \,|\, \psi_p \rangle|^2}{E^{(0)}_p - E^{(0)}_{p'}}$$

with $$\hat{\mu}_m = \beta\,(k\,\hat{L}_m + 2\,\hat{S}_m)$$

where k is a phenomenological parameter to account for the partial ligand character of the metal orbitals.

Because in the following section only the paramagnetic moments of powders are considered, k is chosen to be isotropic. When $\beta H/kT \ll 1$ is not satisfied, the calculation of χ_{mm}, and especially that of the powder magnetization is much more complicated, as has been shown before for d^5 systems[41,42]. For the calculation of the powder magnetization of d^6 compounds, an analogous procedure can be performed, primarily based on (16).

Calculations, Parameters and Results

For the calculation of the energy levels and of the quadrupole splittings the parameters Dq, Ds, Dt, Du, Dv and λ have been introduced. The magnetic susceptibility calculations have an additional parameter k.

A) Relations between Parameters

Thorough theoretical considerations about Ds and Dt, and about their relationships have been given before[39,43,44]. Within a crystalfield model Du/Dv can be related to Ds/Dt: when the effective charges of the ligands on the x, y and z axes are respectively $-Z_1 e$, $-Z_2 e$ and $-Z_3 e$ and the distances to the central atom R_1, R_2 and R_3, then[45,*]

$$Ds = \overline{r^2}\, e^2 (Z_1/R_1{}^3 + Z_2/R_2{}^3 - 2Z_3/R_3{}^3)/7\,, \tag{21}$$

$$Dt = \overline{r^4}\, e^2 (Z_1/R_1{}^5 + Z_2/R_2{}^5 - 2Z_3/R_3{}^5)/21\,, \tag{22}$$

$$Du = -3\,\overline{r^2}\, e^2 (Z_1/R_1{}^3 - Z_2/R_2{}^3)/7\,, \tag{23}$$

$$Dv = 5\,\overline{r^4}\, e^2 (Z_1/R_1{}^5 - Z_2/R_2{}^5)/21\,. \tag{24}$$

When Z_1, Z_2 and Z_3 are equal and the differences of R_1, R_2 and R_3 are small compared to R_1, it can be shown that

$$Du/Dv = -3\,Ds/5\,Dt\,. \tag{25}$$

The same relationship holds when R_1, R_2 and R_3 are equal and the charge differences between Z_1, Z_2 and Z_3 are small compared to Z_1.

From (21) to (24) it can be seen that the common situations will be those, in which Ds and Dt have the same sign and Du has a sign opposite to Dv. The same sign for Ds and Dt is in fact the usually occurring event in practice[39,47,48,49].

B) Discussion of the Results

The course of the curves of the quadrupole splitting ΔE_Q and the magnetic moment μ is determined by the position of the energy levels and the nature of the corresponding eigenfunctions.

For a tetragonal symmetry, Griffith[50] has given the positions of the energy levels of the split $^5T_{2g}$ term, assuming that there is no interaction with the split ^5E_g term. We introduced this interaction, although it does not change dramatically the Griffith's picture of the level positions. Thus, for D_{4h} symmetry we can distinguish two cases:

1) $(3Ds - 5Dt) > 0$. In this case the lowest energy term is ^5E_g, which is split by spin-orbit interaction. This spin-orbit splitting is relatively large: about four times the spin-orbit coupling parameter λ, at least when $(3Ds - 5Dt) \gg |\lambda|$. This large splitting introduces the possibility of a considerable temperature dependence of the paramagnetic and the quadrupole splitting when the temperature increases from 0 to 300 K.
2) $(3Ds - 5Dt) < 0$. The lowest term is $^5B_{2g}$, which is only split by spin-orbit interaction in second order. Therefore the splitting of $^5B_{2g}$ is much smaller than $|\lambda|$, at least when $|3Ds - 5Dt| \gg |\lambda|$. These two situations are shown in Fig. 1.

An additional orthorhombic splitting separates the $|M_L = 1\rangle$ from the $M_L = -1\rangle$ levels, thus splitting the $^5E_g(D_{4h})$ term. See Fig. 1 left and right hand parts.

For calculations presented in Fig. 1, the values of Dq, λ and k were fixed at $Dq = 1000\ \text{cm}^{-1}$, $\lambda = -75\ \text{cm}^{-1}$ and $k = 1.0$. The fixation of λ on $-75\ \text{cm}^{-1}$ means a reduction of the spin-orbit coupling of 30% compared to the free ion value. A reduction of this magnitude has often been found experimentally[11,51,52].

The graphs of powder paramagnetic moments and the absolute values of the quadrupole splitting as a function of temperature are given in Figs. 2 and 3. In these figures the Dt values were fixed by $Ds/Dt = 4$. This means that, according to (25), $Du/Dv = -12/5$. Figure 2 shows the tetragonal case. Since $Ds/Dt = 4$, $3Ds - 5Dt$ has the same sign as Ds. It is shown that the powder paramagnetic moment shows significant temperature dependence

---

[*] We assume an isotropic charge distribution of the central atom and furthermore state that r^2 and r^4 have only significant contribution to r^2 and r^4 for r smaller than R_1. This latter assumption can be derived from Clementi's tables of Atomic Functions[46] for Fe^{2+}.

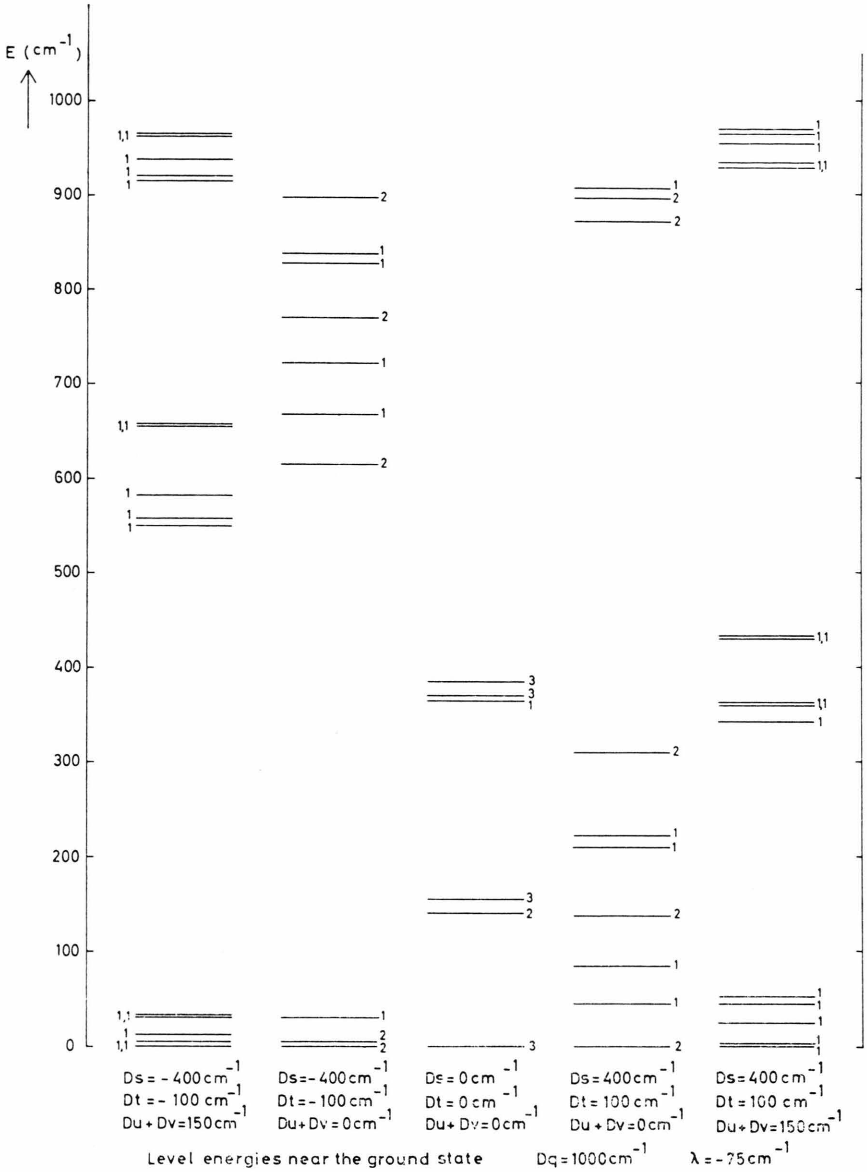

Fig. 1. Energy scheme of low energy levels for an octahedral (centre), tetragonal ($Ds = 400$ cm^{-1}, $Dt = 100$ cm^{-1} and $Ds = -400$ cm^{-1}, $Dt = -100$ cm^{-1}) an orthorhombic symmetry ($Du + Dv = 150$ cm^{-1}).

above 50 K for positive *Ds*, while this is absent for negative *Ds*. Moreover the magnetic moment is lowest for negative *Ds*, because there is no orbital contribution in that case.

Curves for a *k* value lower than 1.0 are not shown. A lower *k* value lowers the powder paramagnetic moment, especially when $(3Ds - 5Dt)$ is positive. In this case a lowering of *k* from 1.0 to 0.7 may lower the powder magnetic moment by 0.25 B.M. The temperature dependence of the curves is also slightly altered in that case.

Concerning the quadrupole splitting, the valence contribution is temperature dependent. This valence contribution is proportional to the ensemble average of $\langle M_L^2 - 2 \rangle$. Therefore, in the tetragonal case, the quadrupole splitting is temperature dependent only when *Ds* is small.

Figure 3 shows the introduction of an additional orthorhombic splitting: $Du = 300$ cm^{-1} and, according to (25), $Dv = -125$ cm^{-1}. As an orthorhombic distortion leads to a splitting of the $^5E_g(D_{4h})$ term, the influence of this distortion on

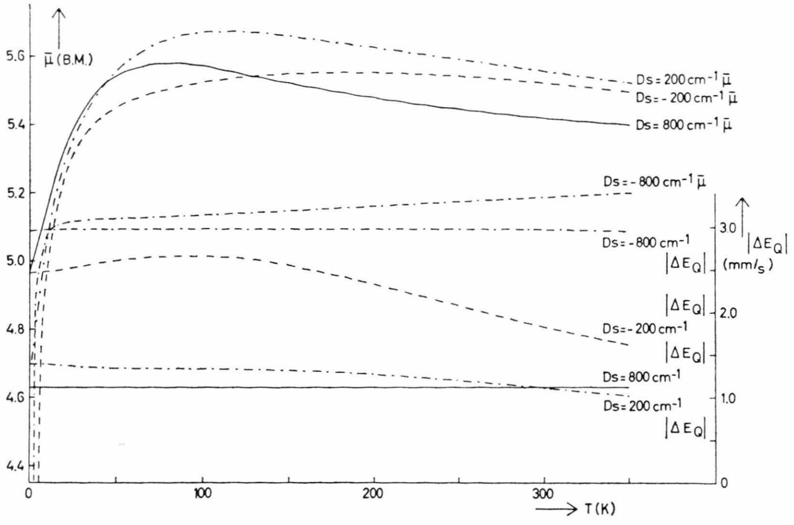

Fig. 2. Powder paramagnetic moments and absolute values of the quadrupole splitting versus temperature. $Ds/Dt = 4$, $Du = Dv = 0$.

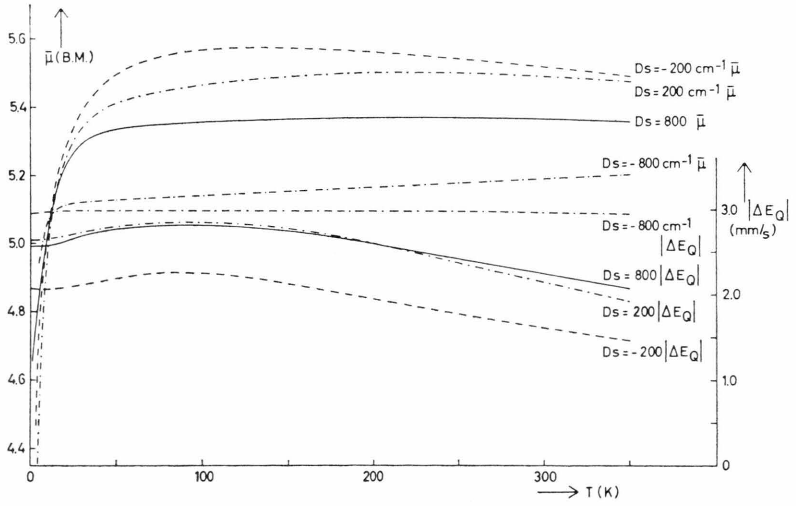

Fig. 3. Powder paramagnetic moments and absolute values of the quadrupole splitting versus temperature. $Ds/Dt = 4$, $Du = 300\ \text{cm}^{-1}$, $Dv = -125\ \text{cm}^{-1}$.

the powder paramagnetic moment and the quadrupole splitting is larger when this $^5E_g(D_{4h})$ term is the ground-state (positive *Ds*). For positive *Ds*, an additional orthorhombic splitting makes that the powder paramagnetic moments are lower, less temperature dependent above 50 K and decreasing sharply below 10 K. The values of the quadrupole splitting for positive *Ds* are higher and more temperature dependent, due to an additional orthorhombic distortion. This is because η is no longer equal to zero.

Figures 4 and 5 show powder paramagnetic moments at 100 K as a function of *Ds* for various *Ds*/*Dt* values. Figure 4 is the tetragonal case. The magnetic moments are highest for $Ds = 0$. The *Ds* and *Dt* ranges are limited by $Dt < 4/7\ Dq$ [39]. The magnetic moment values are — within good accuracy — determined by $3Ds - 5Dt$, the energy separation between $^5B_{2g}(D_{4h})$ and $^5E_g(D_{4h})$, except for such high *Ds* values that the $^5A_{1g}$ term is very low in energy. Figure 5 shows that an additional orthorhombic splitting lowers the magnetic moment at 100 K, especially when $(3Ds - 5Dt)$ is positive.

The values of the quadrupole splitting as a function of *Ds* are shown in Figs 6 and 7. Figure 6 shows the tetragonal case. For $Ds/Dt = 4$ and for $Ds/Dt = 2$, the valence contribution and the lattice contribution to the quadrupole splitting have opposite signs. Therefore these curves have a maximum and

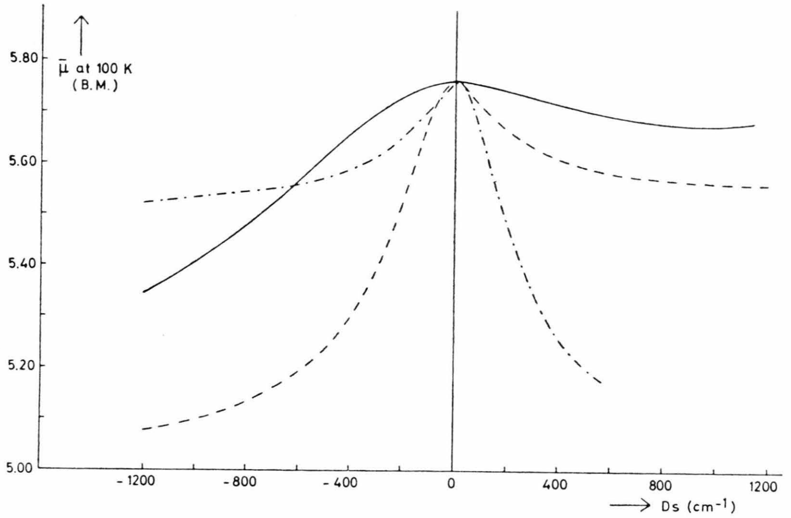

Fig. 4. Powder paramagnetic moments at 100 K versus Ds for various Ds/Dt:
------- $Ds/Dt = 4$,
——— $Ds/Dt = 2$,
–·–·– $Ds/Dt = 1$,
and $Du = 0$, $Dv = 0$.

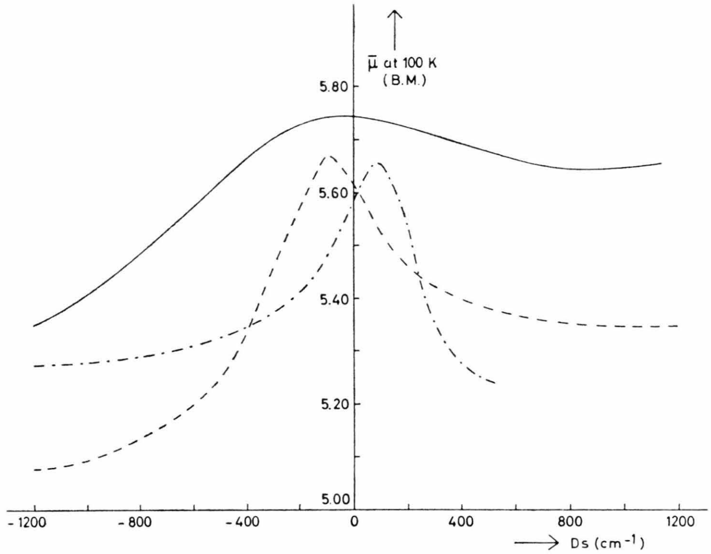

Fig. 5. Powder paramagnetic moments at 100 K versus Ds for various Ds/Dt:
------- $Ds/Dt = 4$,
——— $Ds/Dt = 2$,
–·–·– $Ds/Dt = 1$, and $Du = 300\ \text{cm}^{-1}$, $Dv = -125\ \text{cm}^{-1}$.

a minimum for certain Ds values. For $Ds/Dt = 1$, the valence contribution and the lattice contribution have the same sign, because of the changing of the ground state. Therefore in this case, the quadrupole splitting is a permanently ascending curve. In Figure 7, the absolute value of the quadrupole splitting as a function of Ds has been drawn for an orthorhombicly distorted case. Here the absolute value of the quadrupole splitting has been used, because there is no longer a unique axis that determines the sign. As discussed above, the influence of the orthorhombic distortion is largest when Ds is small or when $3\,Ds - 5\,Dt$ is positive.

Figures 8—11 show level graphs of the quadrupole splitting at 100 K and 300 K with $Ds/Dt = 4$ and $Ds/Dt = 1$. Du values range from 0 to 600 cm^{-1} and Ds from -1200 to 1200 cm^{-1}, or to the value limited by Dt. In these Figures, the curves are dotted in the triangle between $Du = -3\,Ds$ and $Du = 3\,Ds$, because every point within this triangle can, by a transformation of axes, be represented by another point with a lower Du value. The Figures show again that for $Ds/Dt = 1$ higher quadrupole-splitting values are possible than for $Ds/Dt = 4$. When $3\,Ds - 5\,Dt$ is positive it appears that the quadrupole splitting is strongly dependent on the orthorhombic

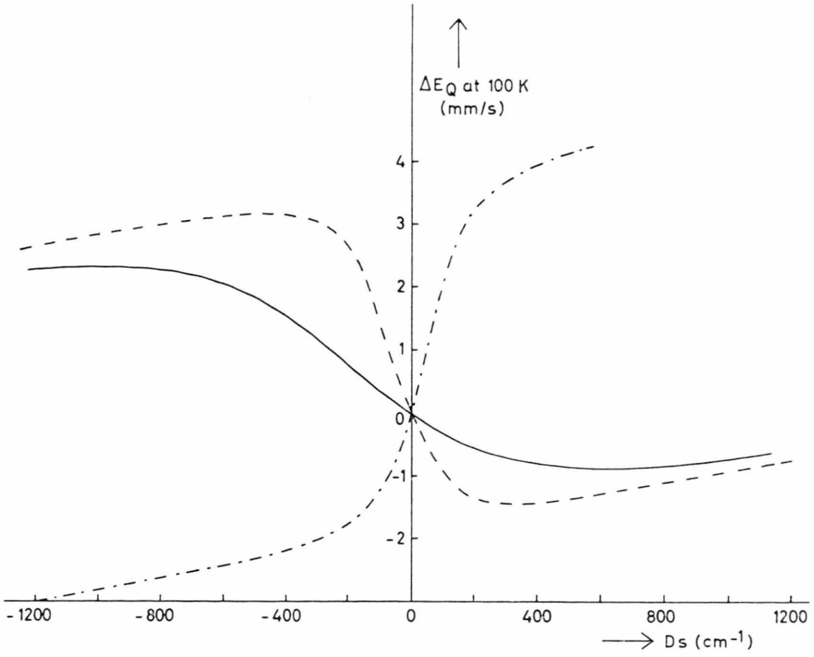

Fig. 6. Quadrupole splittings versus Ds at 100 K vor various Ds/Dt:
------ $Ds/Dt = 4$,
——— $Ds/Dt = 2$,
–·–·– $Ds/Dt = 1$, and $Du = 0$,
$Dv = 0$.

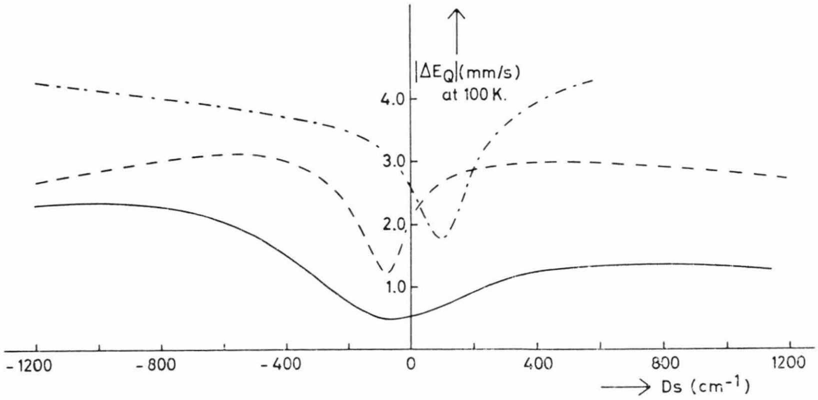

Fig. 7. Absolute values of the quadrupole splitting versus Ds at 100 K for various Ds/Dt:
------ $Ds/Dt = 4$,
——— $Ds/Dt = 2$,
–·–·– $Ds/Dt = 1$, and
$Du = 300\ \mathrm{cm}^{-1}$,
$Dv = 125\ \mathrm{cm}^{-1}$.

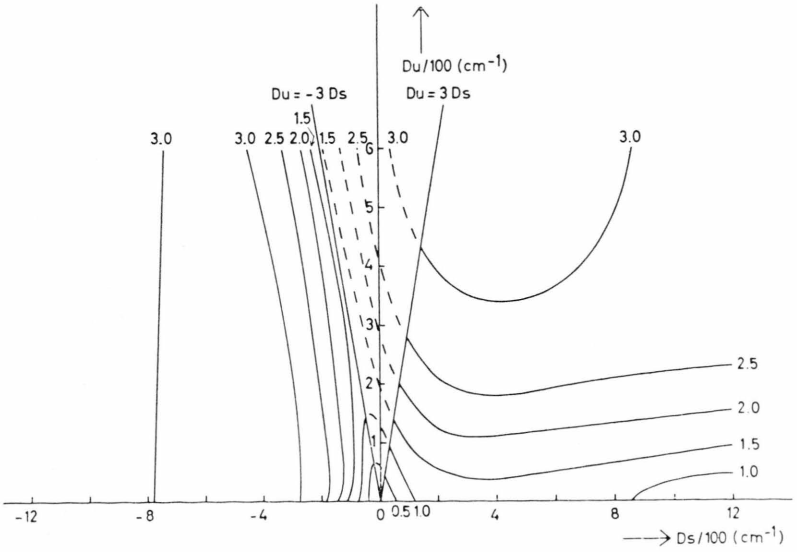

Fig. 8. Level graph of the absolute value of the quadrupole splitting at 100 K. $Ds/Dt = 4$, $Du/Dv = -12/5$.

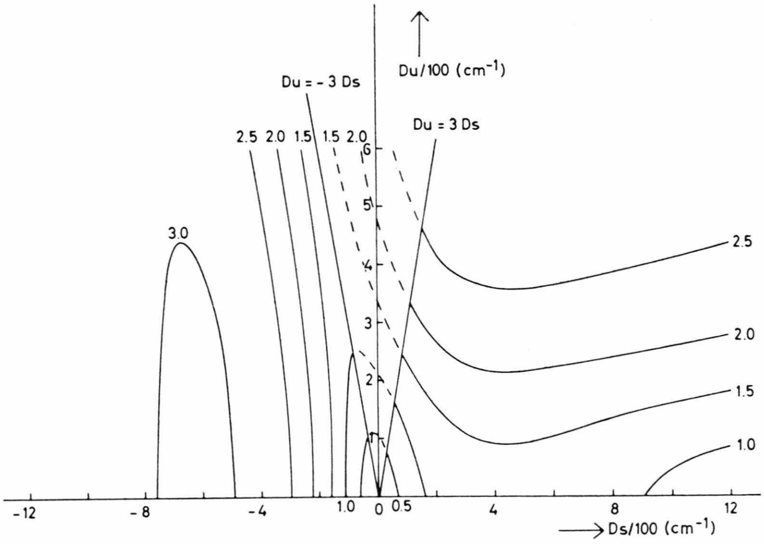

Fig. 9. Level graph of the absolute value of the quadrupole splitting at 300 K. $Ds/Dt = 4$, $Du/Dv = -12/5$.

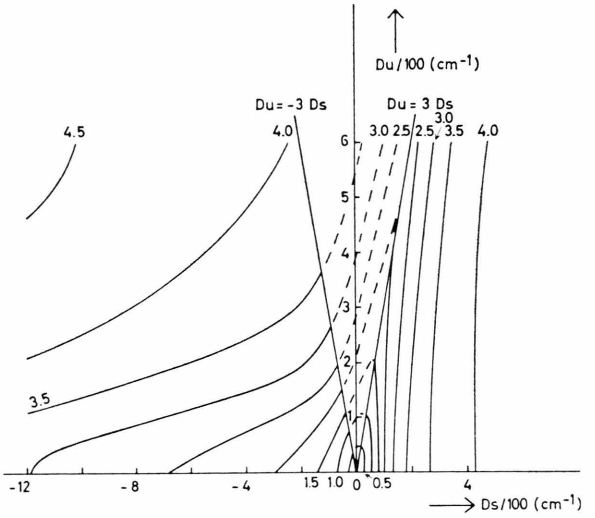

Fig. 10. Level graph of the absolute value of the quadrupole splitting at 100 K. $Ds/Dt = 1$, $Du/Dv = -3/5$.

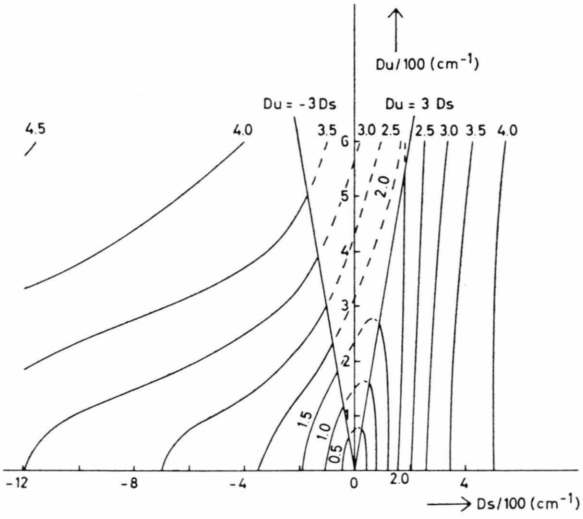

Fig. 11. Level graph of the absolute value of the quadrupole splitting at 300 K. $Ds/Dt = 1$, $Du/Dv = -3/5$.

distortion. Secondly, even for a small orthorhombic distortion, the total calculated quadrupole splitting may differ significantly from the algebraic sum of the lattice- and the valence-quadrupole splitting. Therefore, some calculations performed in the past[8,9,11] are probably less accurate.

If we compare the present results of the powder magnetic moment and the quadrupole splitting with those obtained by others[1,2,4], some further remarks can be made:

i) The inclusion of the $^5E_g(O_h)$ term in theory, especially influences the results of the magnetic susceptibility. This inclusion permits a partial removal of the quenching of the orbital angular momentum by second-order spin-orbit interaction and gives an additional contribution to the second-order Zeeman effect. Therefore, the powder paramagnetic moments calculated by the present theory, are higher than those obtained by others[1,2]. These differences vary, for $Dq = 1000\ \text{cm}^{-1}$, from 0.03 to 0.15 B.M.

The actual differences depend on the values of the distortion parameters and the temperature.

ii) On the other hand, the inclusion of this $^5E_g(O_h)$ term, hardly influences the results of the quadrupole splitting. For $Dq = 1000\ \mathrm{cm}^{-1}$, the differences are less than 2%.

iii) When, contrary to Ingall's work, Dt and Dv are not ignored, the theory of the quadrupole splitting is also applicable to compounds, having Dt values of the same order of magnitude as Ds[6,8,11].

Considering the results derived in this paper, one may question about their applicability on fitting experimental data. It is clear that measurements of magnetic anisotropy and Mössbauer spectra in an applied magnetic field at distinct temperatures yield most useful information to compare with an extended theoretical model as derived above. The best way to evaluate the validity of this model or to apply the model to a particular compound, is to perform these types of measurements. However, the routine use of these techniques is possible only in a few laboratories, whereas simple poweder susceptibility and Mössbauer facilities are much more common. These measurements are especially useful for comparison within a series of structurally related compounds. Especially for the interpretation of this type of measurements the present study has been done, and the results presented in the figures have been attuned to this purpose. As mentioned before, the way in which the lattice contribution to the quadrupole splitting is calculated, is especially suitable for a simultaneous investigation of a series of isostructural compounds. Concerning the powder paramagnetic moment we admit that these magnetic generally will yield insufficient information to derive accurate conclusions for a single compound[53]. But in combination with other kinds of certain measurements and in the study of a series of compounds, much more informative conclusions are allowed. The comparison between the present theory and the measurements of a series of related compounds, will be made in the following paper[54].

[1] B. N. Figgis, J. Lewis, F. E. Mabbs, and G. A. Webb, J. Chem. Soc. (A) **1967**, 442.

[2] E. König, A. S. Chakravarty, and K. Madeja, Theor. Chim. Acta (Berl.) **9**, 151 [1967]; **9**, 171 [1967].

[3] M. Gerloch, J. Lewis, and W. R. Smail, J. C. S. Dalton **14**, 1559 [1972].

[4] R. Ingalls, Phys. Rev. **133**, A787 [1964].

[5] R. M. Golding, K. F. Mok, and J. F. Duncan, Inorg. Chem. **5**, 774 [1966].

[6] C. D. Burbridge, D. M. L. Goodgame, and M. Goodgame, J. Chem. Soc. (A) **1967**, 349.

[7] R. Ingalls, K. Ono, and Louis Chandler, Phys. Rev. **172**, 295 [1968].

[8] P. B. Merrithew, P. G. Rasmussen, and D. H. Vincent, Inorg. Chem. **10**, 1401 [1971].

[9] J. Reedijk and D. W. Engelfriet, Rec. Trav. Chim. **91**, 883 [1972].

[10] J. F. K. M. de Vries, Thesis, Nijmegen 1972.

[11] P. B. Merrithew, J. J. Guerrera, and A. J. Modestino, Inorg. Chem. **13**, 644 [1974].

[12] T. C. Gibb, J. Chem. Soc. (A) **1968**, 1439.

[13] M. T. Hutchings, Solid State Physics **16**, 227 [1964].

[14] C. J. Ballhausen, Introduction to Ligand Field Theory, McGraw-Hill Book Company, New York 1962.

[15] T. Lulek, Acta Phys. Polon. **A40**, 797 [1971].

[16] T. Lulek, Acta Phys. Polon. **A43**, 705 [1973].

[17] O. Kahn and S. F. A. Kettle, Theor. Chim. Acta **27**, 187 [1972].

[18] O. Kahn and S. F. A. Kettle, Theor. Chim. Acta **29**, 359 [1973].

[19] O. Kahn and S. F. A. Kettle, Mol. Phys. **29** (1), 61 [1975].

[20] R. W. Balk, unpublished results.

[21] J. R. Sams and T. B. Tsin, Inorg. Chem. **14**, 1573 [1975].

[22] J. Reedijk, F. W. Klaaijsen, and H. T. Witteveen, J. Chem. Soc., Faraday Trans. (II) **69**, 1537 [1973].

[23] R. D. Dowsing, B. Nieuwenhuijse, and J. Reedijk, Inorg. Chim. Acta **5**, 301 [1971].

[24] V. R. Marathe and S. Mitra, Chem. Phys. Letters **21**, 62 [1973].

[25] M. H. Cohen and R. Reif, Solid State Physics **5**, 321 [1957].

[26] A. J. Nozik and M. Kaplan, Phys. Rev. **159** (2), 273 [1967].

[27] J. O. Artman, A. H. Muir, and H. Widersich, Phys. Rev. **173**, 337 [1968].

[28] J. M. Friedt and J. Inorg. Nucl. Chem. **32** (2), 431 [1970].

[29] H. R. Leider and D. N. Pipcorn, Phys. Rev. **165**, 494 [1968].

[30] J. Chappert, R. B. Frankel, A. Misetich, and N. A. Blum, Phys. Letters **28B**, 406 [1968/1969].

[31] J. M. Friedt, Proc. Conf. Appl. Mössb. Effect (Tihany, 1969).

[32] R. R. Sharma, Phys. Rev. Letters **26** (10), 563 [1971].

[33] A. Trautwein and Frank E. Harris, Phys. Rev. **B7** (11), 4755 [1973].

[34] A. J. Freeman and R. E. Watson, Phys. Rev. **131**, 2566 [1963].

[35] R. Ingalls, Phys. Rev. **188**, 1045 [1969].

[36] D. P. Johnson and R. Ingalls, Phys. Rev. **B1**, 1013 [1970].

[37] R. B. Frankel, J. Chappert, J. R. Regnard, A. Misetich, and C. R. Abeledo, Phys. Rev. **B5**, 2469 [1972].

[38] M. G. Clark, G. M. Bancroft, and A. J. Stone, J. Chem. Phys. **47**, 4250 [1967].

[39] M. Gerloch and R. C. Slade, Ligand Field Parameters, Cambridge University Press [1973].

[40] T. F. Soules, J. W. Richardson, and D. M. Vaught, Phys. Rev. **B3**, 2186 [1971].

[41] V. R. Marathe and S. Mitra, Chem. Phys. Letters **27**, 103 [1974].

[42] A. Vermaas and W. L. Groeneveld, Chem. Phys. Letters **27**, 583 [1974].

[43] A. B. P. Lever, Coord. Chem. Rev. **3**, 119 [1968].

[44] A. B. P. Lever, B. R. Hollebone, and J. C. Donini, J. Amer. Chem. Soc. **93**, 6455 [1971].

[45] S. Sugano, Y. Tanabe, and H. Kamimura, Multiplets of Transition Metal Ions in Crystals, Academic Press, New York 1970.

[46] E. Clementi, IBM Journal of Research and Development **9**, 2 [1965].

[47] D. A. Rowley and R. S. Drago, Inorg. Chem. **7**, 795 [1968].

[48] R. L. Chiang and R. S. Drago, Inorg. Chem. **10**, 453 [1971].

[49] J. Reedijk, Rec. Trav. Chim. **89**, 605 [1970].

[50] J. S. Griffith, The Theory of Transition Metal Ions, Cambridge University Press 1961, p. 357.

[51] M. Gerloch, J. W. Lewis, and W. R. Smail, J. Chem. Soc. (A) [1971], 2434.

[52] A. Vermaas, W. L. Groeneveld, and J. Reedijk, Z. Naturforsch. **32a**, 632 [1977].

[53] A. K. Gregson and S. Mitra, Chem. Phys. Letters **3**, 528 [1969].

[54] A. Vermaas, W. L. Groeneveld, and J. Reedijk, Part II, following paper.